

Peptide-Mediated Blood–Brain Barrier Transport of Polymersomes**

Julia V. Georgieva, René P. Brinkhuis, Katica Stojanov, Carel A. G. M. Weijers, Han Zuilhof, Floris P. J. T. Rutjes, Dick Hoekstra, Jan C. M. van Hest,* and Inge S. Zuhorn*

The effective treatment of brain-related diseases is severely hampered by the presence of the blood–brain barrier (BBB), a polarized layer of endothelial cells that physically separates blood from brain tissue.^[1] Besides being able to cross the BBB, drugs must display sufficient stability and bioavailability.^[2] Once drugs have reached the brain side, they are exposed to multidrug resistance receptors on the endothelial cell surface to rapidly clear them from the brain.^[3] These obstacles can be overcome by the application of nanocarriers, provided that they are effectively targeted to this endothelial cell layer, and that they subsequently engage in transcytosis across the BBB, thus leading to their entry into brain tissue.

The best studied nanocarriers for drug delivery over the BBB are liposomes, which have been decorated^[4] with antibodies, proteins,^[5] or peptides^[6] derived from protein-binding domains.^[7] However, all targeted liposomes showed only a limited association with the BBB in vivo as was shown by van Rooy et al.^[5] Only liposomes conjugated to transferrin antibody RI7217—having a molecular weight of 90 kg mol^{−1}—were able to significantly enhance the uptake by the brain.

A relatively new class of nanocarriers consists of polymeric vesicles or polymersomes,^[8] which self-assemble in aqueous media from amphiphilic block copolymers. They resemble liposomes in their basic morphology, but have as

a clear difference a thicker bilayer membrane which can be 100 percent PEGylated; PEG = poly(ethylene glycol). This renders them considerably more stable than liposomes, and improves the blood circulation ability.^[9] Furthermore, the larger apolar compartment of polymersomes as compared to liposomes allows a higher loading of hydrophobic drugs. Since the majority of central nervous system (CNS) drugs is hydrophobic, there is a large added value in preparing polymeric carriers for efficient transport over the BBB into the brain. Until now, only one research group reported polymersomes for targeted transport over the BBB. In these studies polymersomes were tagged with transferrin^[10] or RI7217^[11] analogous to liposomes. Clearly, to develop efficient nanocarrier systems a broader choice in selective targeting units and receptors is required. Moreover these targeting units should still be active when conjugated to the polymersome surface and preferentially have a low molecular weight for simple synthesis and conjugation.

Herein we report the design and synthesis of a polymersome nanocarrier, tagged with a dodecamer peptide of only 1645 g mol^{−1}, which is able to efficiently cross the BBB, both in vitro and in vivo. The peptide G23 was identified by means of phage display with ganglioside GM1 as target. Although the G23 peptide has previously been reported for binding to gangliosides,^[12] it has now been employed for the first time to promote transport of nanocarriers over the BBB (Figure 1).

The block copolymers for the formation of polymersomes are depicted in Scheme 1. Details on the synthetic procedures can be found in the Supporting Information. We chose to

[*] R. P. Brinkhuis,^[†] Prof. Dr. F. P. J. T. Rutjes, Prof. Dr. J. C. M. van Hest
Radboud University Nijmegen, Institute for Molecules and Materials
Heyendaalseweg 135, 6525AJ Nijmegen (The Netherlands)
E-mail: j.vanhest@science.ru.nl

J. V. Georgieva,^[†] K. Stojanov, Prof. Dr. D. Hoekstra, Dr. I. S. Zuhorn
Department of Cell Biology, Section Membrane Biology
University Medical Center Groningen, Groningen University
A. Deusinglaan 1, 9713AV Groningen (The Netherlands)
E-mail: i.zuhorn@umcg.nl

Dr. C. A. G. M. Weijers, Prof. Dr. H. Zuilhof
Laboratory of Organic Chemistry, Wageningen University
Dreijenplein 8, 6703 HB Wageningen (The Netherlands)
and
Department of Chemical and Materials Engineering
King Abdulaziz University, Jeddah (Saudi Arabia)

[†] These authors contributed equally to this work.

[**] This work was performed within the framework of the Dutch Top Institute Pharma project number T5-105. Hans Adams is acknowledged for his help with peptide synthesis. Microscopy imaging was performed at the UMCG Imaging Center (UMIC), supported by the Netherlands Organisation for Health Research and Development (ZonMW grant 40-00506-98-9021).

Supporting information for this article is available on the WWW under <http://dx.doi.org/10.1002/anie.201202001>.

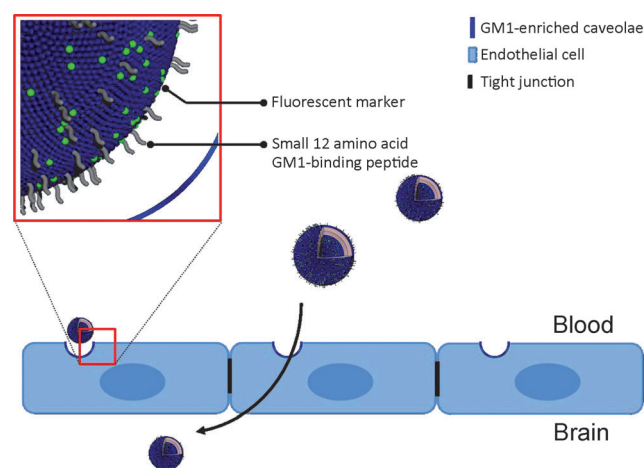
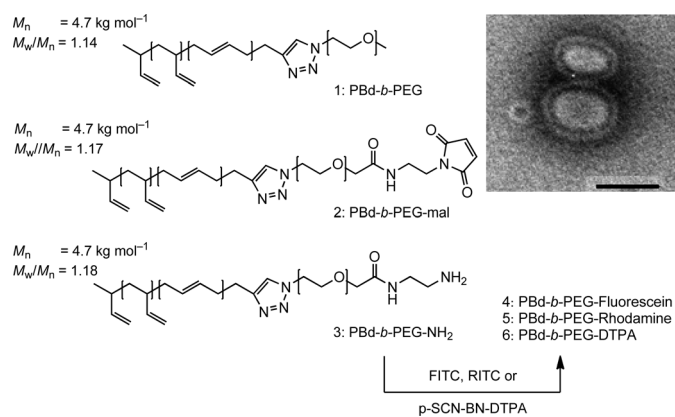


Figure 1. Polymeric vesicles tagged with a small peptide that recognizes GM1-enriched caveolae which serve as transcytotic entry portal. These polymersomes are able to efficiently cross the BBB into the brain parenchyma as shown herein, opening new routes toward effective treatment of brain-related diseases.



Scheme 1. Left side: Amphiphilic block copolymers used in this study. Polymer 1 is the main building block of the polymersomes. Polymer 2 is a maleimide-functionalized analog to couple peptides. Starting from polymer 3, fluorescein, rhodamine, and DTPA end-functionalized analogs were obtained. Right side: TEM picture of polymersomes formed from 1, 2, and 4 in a ratio of 8:1:1. The black bar represents 200 nm.

work with amphiphilic block copolymers (1) consisting of polybutadiene and PEG mainly for two reasons. First of all, this block copolymer is generally considered to be biocompatible, and secondly the low glass-transition temperature of polybutadiene allows for extrusion—and therefore resizing—of the polymersomes. This has been shown to be of great importance for long in vivo circulation.^[13] Furthermore, PEG induces stealth behavior of the vesicles and therefore prevents cell adhesion as well as opsonisation and thereby recognition by the reticulo endothelial system (RES). To functionalize the polymersomes with targeting peptides, maleimide end groups were introduced (2). As a tracing moiety, either fluorescein (4), rhodamine (5), or diethylenetriamine pentaacetate (DTPA) (6) was introduced in polymer 3 through isothiocyanate derivatives of the tracer.

Peptides that were known before this study to target the BBB were limited to the trans-activating transcriptional activator (Tat) peptide,^[6] opioid-derived peptides,^[14] and the bigger RVG-9R peptide,^[7] which all showed limited in vivo delivery into the brain parenchyma.^[15] To identify potentially more potent peptides, we considered that caveolae, which are present on the luminal surface of endothelial cells, are well-known as cellular entry portals for transcytotic transport.^[16] Since caveolae are enriched in GM1, we reasoned that this could be an appropriate target to mediate transport into the brain. We therefore performed a phage library selection, using the Ph.D-12 library from BioLabs with immobilized GM1 as target.^[17] After three panning rounds 20 plaques were selected of which three plaques shared the sequence defined as G23. We selected the peptides defined as G23 and G88 based on their efficient binding and homogeneous patterning upon interaction of the phages with human cerebral microvascular endothelial cells (hCMEC/D3).^[18] The selected peptides were synthesized through standard 9-fluorenylmethoxycarbonyl (Fmoc) chemistry with an additional C-terminal cysteine.

Polymersomes were prepared by mixing block copolymers 1, 2, and 4 (8:1:1) for all in vitro studies (Table 1). The

Table 1: Characteristics of polymersome samples used for in vivo and in vitro studies.

ID/Peptide ^[a]	Sequence ^[b]	Size [PDI]	Charge ^[c]	Zeta ^[d]
Non _{fluor}	—	220 (0.11)	—	−6.32
G88 _{fluor}	NPAGPSPAHIIISC	220 (0.11)	−0.8	−14.59
G23 _{fluor}	HLNILSTLWKYRC	220 (0.11)	+1.8	−1.70
Scr _{fluor}	KISHLLNYRTWLC	228 (0.10)	+1.8	−2.83
G23(5%) _{fluor}	HLNILSTLWKYRC	227 (0.12)	+1.8	−3.21
Non _{rhod}	—	164 (0.10)	—	−2.64
G23 _{rhod}	HLNILSTLWKYRC	165 (0.12)	+1.8	−8.42

[a] The samples contain 10 mol % fluorescently labelled polymer (fluor = fluorescein, rhod = rhodamine), 10% of the surface is covered with peptides. [b] Peptide sequences with C-terminal cysteine for coupling to the polymersome surface. [c] Formal charge at pH 7.8. [d] Measured in water (pH 7.8) with an applied potential of 24 V.

polymeric vesicles were formed through the solvent switch method, after which they were extruded to an average size of 220 nm with a polydispersity index (PDI) of 0.11. The selected peptides were coupled through cysteine/maleimide chemistry, starting from the same batch of maleimide-functionalized polymersomes. The zeta potentials showed in all cases a clear change in surface charge after the coupling of peptides (Table 1). For in vivo experiments polymersomes were prepared with rhodamine as tracer, thus combining polymers 1, 2, and 5 (8:1:1). The polymersomes were reduced in size to 165 nm, to allow sufficiently long blood circulation to enable accumulation in the brain vasculature, yet short enough to prevent false comparison of targeted and nontargeted particles because of a big difference in blood clearance.^[13b]

The transcytosis capacity of targeted and nontargeted polymersomes was determined in hCMEC/D3 cells, cultured on transwell filters (Figure 2c). The hCMEC/D3 cell line is a good model for the human blood–brain barrier.^[18,19]

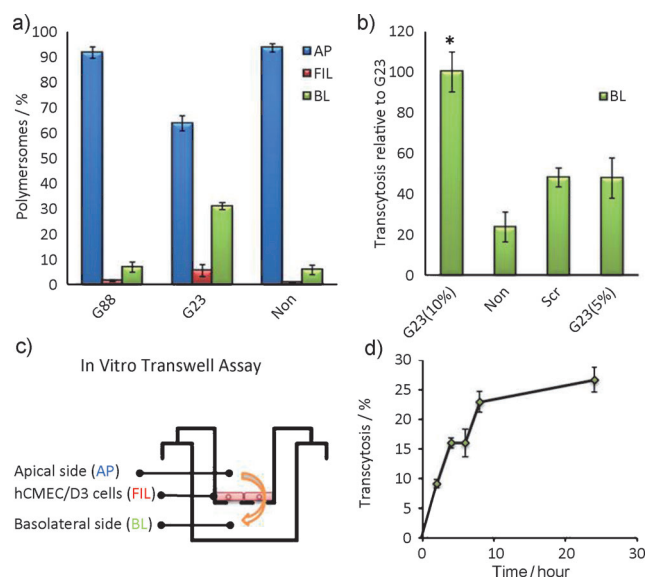


Figure 2. a) In vitro transcytosis capacity of polymersomes functionalized with the selected peptides. b) Scrambling of the G23 sequence and lowering the surface functionalization with G23 both resulted in reduced in vitro transcytosis. c) Schematic overview of the in vitro hCMEC/D3 cell transwell assay. d) Kinetic plot of in vitro G23-mediated transcytosis of polymersomes.

Recently this approach has also been used by Ragnai et al.^[20] to study the transcytosis of SiO₂ nanoparticles. Fluorescently labeled polymersomes were added to the apical side of the polarized endothelial monolayer and incubated for 18 h at 37°C, after which the percentages of the total applied dose in the apical chamber (AP), basolateral chamber (BA), and cellular monolayer (FIL) were determined by means of fluorescence spectroscopy.

As evident from Figure 2a, the G23 polymersomes showed the most prominent transcytotic capacity. Specifically, (30.8 ± 1.4) % of the G23 polymersomes were recovered at the basolateral side. This implies on average a more than four-fold increase in the transcytotic capacity, compared to the basolateral recovery of nontargeted polymersomes (5.7 ± 0.8%), or polymersomes tagged with G88 (6.8 ± 1.9%). In addition to a highly efficient appearance in the basolateral medium, the G23 polymersomes showed an enhanced association with the cells (Figure 2a; G23; FIL). Thus, (5.5 ± 2.3) % of the added dose remained cell-associated, representing two–three times as much as the cellular association of the other polymersome preparations tested. These data emphasize the specific role of G23 in mediating the observed transcytotic transport, and exclude potential leakiness of the cell monolayer, as this should have resulted in a nonspecific appearance of polymersomes in the basolateral medium. The specificity of G23-mediated transport was further supported by determining the kinetics of transcytosis of the G23 polymersomes across hCMEC/D3 cells. As shown in Figure 2d, typical saturation kinetics were obtained, supporting the involvement of an active, receptor-mediated pathway, possibly reflecting differences in the kinetics of transcytosis and recycling of the receptor(s).

To investigate a potential correlation between physicochemical properties (e.g. charge and hydrophobicity) and transcytotic capacity of the peptide, a scrambled version of the G23 peptide (Scr) polymersomes was prepared and compared to “native” G23 and nontargeted polymersomes. As illustrated in Figure 2b a twofold reduction in transcytosis across the *in vitro* BBB model was observed between Scr polymersomes and G23-targeted polymersomes. Next, the peptide density was reduced from 10 to 5 mol%. Lowering the incorporation of G23 also led to a twofold reduction in transcytosis (Figure 2b). Together, these data strongly support the view that the G23 peptide, when coated on the surface of polymersomes, displays a specific capacity in mediating their transport across polarized hCMEC/D3 cells.

Although G23 was specifically selected for GM1 as its targeting receptor, the peptide was reported to bind to a structurally similar ganglioside GT1b^[12a] and to displace its natural ligand tetanus toxin C.^[21] Together with this study this binding behavior clearly indicates that G23 recognizes at least two gangliosides. We therefore considered that gangliosides GD1a, GD1b, and/or GT1b, which except for additional sialic acid residues are structurally closely related to GM1 (see Figure S1 in the Supporting Information), may also function as receptors. When GM1, the related gangliosides GD1a, GD1b, and GT1b as well as the unrelated gangliosides GM2, GM3, and GD3—spotted on a dot blot—were incubated with radioactively labeled G23 polymersomes, binding only oc-

curred to GM1 and GT1b. These data thus suggest that next to GM1, GT1b also might act as a cellular receptor for the G23-coupled polymersomes. Next, we determined whether the binding of G23 polymersomes to GT1b also occurs in a cellular context by establishing the extent of colocalization between GT1b, as visualized by immunostaining, and fluorescently labeled G23 polymersomes. Colocalization of G23 polymersomes with GT1b was (16.2 ± 6.4) %, whereas colocalization with GD1a was less than 3 % (see Figure S8 in the Supporting Information).

To reveal the potential of G23 to also mediate the BBB passage *in vivo*, rhodamine-labeled G23 polymersomes and nontargeted polymersomes were administered by intracarotid artery injection in BALB/c mice. The brain distribution of both rhodamine-labeled polymersomes was then analyzed 24 h after injection by preparing thin brain slices as described in detail in the Supporting Information. The brain microvessels were visualized by staining for the platelet endothelial cell adhesion molecule (PECAM, CD31), while the nuclei were stained with 4',6-diamidino-2-phenylindole (DAPI). As demonstrated in Figure 3 nontargeted polymersomes were absent in the brain parenchyma (left panel), while significant

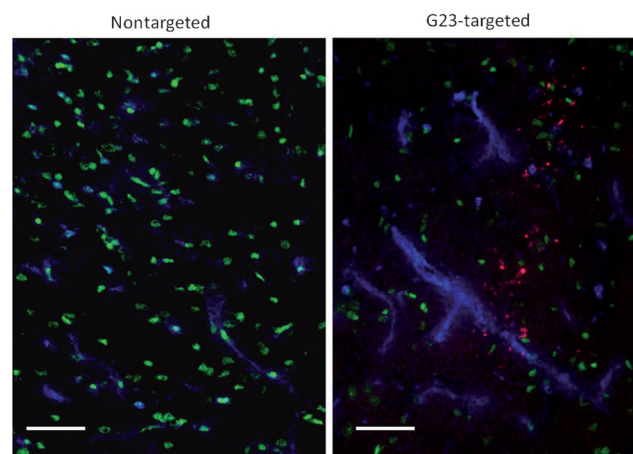


Figure 3. *In vivo* brain distribution of polymersomes after intracarotid artery injection in mice. BALB/c mice were injected with G23 and nontargeted polymersomes. 24 h after injection the brains were isolated and processed as specified in the Supporting Information. In contrast to the absence of nontargeted polymersomes in brain parenchyma (left panel), significant accumulation of G23 polymersomes was found (right panel). Polymersomes are pseudocolored in red, CD31 (brain microvessels) in blue, and nuclei in green. The scale bars are 50 μ m.

accumulation was found for G23 polymersomes (right panel). In depth analysis of all brain slices also revealed accumulation of G23 polymersomes in the cortex, striatum (forebrain), midbrain, pons, and cerebellum. In marked contrast, nontargeted polymersomes were only found in the leaky vessels of the fourth ventricle, ependymal cells of the aqueduct and only occasionally in brain parenchyma.

In conclusion, we have identified the low-molecular-weight peptide, G23, which when coupled to polymeric vesicles, binds to cell-surface-localized gangliosides GM1

and GT1b. By doing so it is able to mediate the transport of nanocarriers over the blood–brain barrier both in vitro and in vivo. The combination of the low-molecular-weight G23 peptide, targeting GM1/GT1b receptors, the robust polymeric carrier and the efficient in vitro and in vivo transcytosis is unprecedented and therefore adds new possibilities to the development of efficient drug nanocarriers for the treatment of brain and CNS-related diseases.

Received: March 13, 2012

Revised: June 20, 2012

Published online: July 11, 2012

Keywords: bioorganic chemistry · blood–brain barrier · drug delivery · peptides · polymersomes

- [1] W. M. Pardridge, *Drug Discovery Today* **2007**, *12*, 54–61.
- [2] R. Duncan, *Nat. Rev. Drug Discovery* **2003**, *2*, 347–360.
- [3] R. Cecchelli, V. Berezowski, S. Lundquist, M. Culot, M. Renftel, M. P. Dehouck, L. Fenart, *Nat. Rev. Drug Discovery* **2007**, *6*, 650–661.
- [4] a) H. J. Lee, B. Engelhardt, J. Lesley, U. Bickel, W. M. Pardridge, *J. Pharmacol. Exp. Ther.* **2000**, *292*, 1048–1052; b) R. J. Boado, Y. F. Zhang, Y. Zhang, W. M. Pardridge, *Biotechnol. Bioeng.* **2007**, *96*, 381–391; c) K. Ulbrich, T. Knobloch, J. Kreuter, *J. Drug Targeting* **2011**, *19*, 125–132; d) E. Garcia-Garcia, K. Andrieux, S. Gil, P. Couvreur, *Int. J. Pharm.* **2005**, *298*, 274–292.
- [5] I. van Rooy, E. Mastrobattista, G. Storm, W. E. Hennink, R. M. Schiffelers, *J. Controlled Release* **2011**, *150*, 30–36.
- [6] a) L. H. Liu, S. S. Venkatraman, Y. Y. Yang, K. Guo, J. Lu, B. P. He, S. Mochhala, L. J. Kan, *Biopolymers* **2008**, *90*, 617–623; b) S. R. Schwarze, A. Ho, A. Vocero-Akbani, S. F. Dowdy, *Science* **1999**, *285*, 1569–1572.
- [7] P. Kumar, H. Q. Wu, J. L. McBride, K. E. Jung, M. H. Kim, B. L. Davidson, S. K. Lee, P. Shankar, N. Manjunath, *Nature* **2007**, *448*, 39–43.
- [8] a) B. M. Discher, Y. Y. Won, D. S. Ege, J. C. M. Lee, F. S. Bates, D. E. Discher, D. A. Hammer, *Science* **1999**, *284*, 1143–1146; b) R. P. Brinkhuis, F. P. J. T. Rutjes, J. C. M. van Hest, *Polym. Chem.* **2011**, *2*, 1449–1462.
- [9] P. J. Photos, L. Bacakova, B. Discher, F. S. Bates, D. E. Discher, *J. Controlled Release* **2003**, *90*, 323–334.
- [10] Z. Q. Pang, H. L. Gao, Y. Yu, J. Chen, L. R. Guo, J. F. Ren, Z. Y. Wen, J. H. Su, X. G. Jiang, *Int. J. Pharm.* **2011**, *415*, 284–292.
- [11] Z. Q. Pang, W. Lu, H. L. Gao, K. L. Hu, J. Chen, C. L. Zhang, X. L. Gao, X. G. Jiang, C. Q. Zhu, *J. Controlled Release* **2008**, *128*, 120–127.
- [12] a) J. K. Liu, Q. S. Tenga, M. Garrity-Moses, T. Federici, D. Tanase, M. J. Imperiale, N. M. Boulis, *Neurobiol. Dis.* **2005**, *19*, 407–418; b) Y. Zhang, W. Zhang, A. H. Johnston, T. A. Newman, I. Pyykko, J. Zou, *Int. J. Nanomedicine* **2012**, *7*, 1015–1022.
- [13] a) Y. Anraku, A. Kishimura, A. Kobayashi, M. Oba, K. Kataoka, *Chem. Commun.* **2011**, *47*, 6054–6056; b) R. P. Brinkhuis, K. Stojanov, P. Laverman, J. Eilander, I. S. Zuhorn, P. J. T. Rutjes, J. C. M. Hest, *Bioconjugate Chem.* **2012**, *23*, 958–965.
- [14] L. Costantino, F. Gandolfi, G. Tosi, F. Rivasi, M. A. Vandelli, F. Forni, *J. Controlled Release* **2005**, *108*, 84–96.
- [15] I. van Rooy, S. Cakir-Tascioglu, W. E. Hennink, G. Storm, R. M. Schiffelers, E. Mastrobattista, *Pharm. Res.* **2011**, *28*, 456–471.
- [16] R. R. Sprenger, R. D. Fontijn, J. van Marle, H. Pannekoek, A. J. G. Horrevoets, *Biochem. J.* **2006**, *400*, 401–410.
- [17] A. V. Pukin, C. A. G. M. Weijers, B. van Lagen, R. Wechselberger, B. Sun, M. Gilbert, M. F. Karwaski, D. E. A. Florack, B. C. Jacobs, A. P. Tio-Gillen, A. van Belkum, H. P. Endtz, G. M. Visser, H. Zuilhof, *Carbohydr. Res.* **2008**, *343*, 636–650.
- [18] B. B. Weksler, E. A. Subileau, N. Perriere, P. Charneau, K. Holloway, M. Leveque, H. Tricoire-Leignel, A. Nicotra, S. Bourdoulous, P. Turowski, D. K. Male, F. Roux, J. Greenwood, I. A. Romero, P. O. Couraud, *Faseb J.* **2005**, *19*, 1872–1876.
- [19] J. V. Georgieva, D. Kalicharan, P. O. Couraud, I. A. Romero, B. Weksler, D. Hoekstra, I. S. Zuhorn, *Mol. Ther.* **2011**, *19*, 318–325.
- [20] M. N. Ragnail, M. Brown, D. Ye, M. Bramini, S. Callanan, I. Lynch, K. A. Dawson, *Eur. J. Pharm. Biopharm.* **2011**, *77*, 360–367.
- [21] T. Federici, J. K. Liu, Q. Teng, J. Yang, N. M. Boulis, *Neurosurgery* **2007**, *60*, 911–918.